Eur. Phys. J. Plus (2017) **132**: 134
DOI 10.1140/epjp/i2017-11411-3

THE EUROPEAN PHYSICAL JOURNAL PLUS

Regular Article

Construction of the energy matrix for complex atoms

Part VII: High-performance computing in the case of terbium atom

Magdalena Elantkowska[1,a], Andrzej Sikorski[2], Jarosław Ruczkowski[2], and Jerzy Dembczyński[2]

[1] Institute of Materials Research and Quantum Engineering, Faculty of Technical Physics, Poznan University of Technology, Piotrowo 3, 60-965 Poznań, Poland
[2] Institute of Control and Information Engineering, Faculty of Electrical Engineering, Poznan University of Technology, Piotrowo 3A, 60-965 Poznań, Poland

Received: 25 January 2017 / Revised: 14 February 2017
Published online: 22 March 2017

Abstract. We report the fine structure analysis of the even configurations system of atomic terbium in the complete set of $4f^N$-core states. For the purpose of the huge matrix diagonalization, we propose the methods utilizing the personal computer clusters and, alternatively, the Microsoft Azure cloud computing. The implementation of these approaches is presented.

1 Introduction

The present paper is the seventh one in the series of our systematic investigations on the structure of complex atom. The six of previous works entitled *Construction of the energy matrix for complex atoms* can be characterized as follows:

- Part I: general remarks on our method of semi-empirical analysis of complex atoms [1].
- Part II: introduction of the explicit formulae for inter-configuration interactions between the configurations containing up to four open shells [2].
- Parts III and IV: discussion of effective electrostatic interactions caused by the excitation of two equivalent electrons, as well as of one electron from a closed shell into an open shell or an empty shell [3,4].
- Part V: discussion of electrostatically correlated spin-orbit interactions, as well as electrostatically correlated hyperfine interactions caused by the excitation of one electrons from a closed shell into an open shell or an empty shell [5].
- Part VI: discussion of contributions to the hyperfine structure originating from core polarization effects [6].

The aim of this paper is the application of our semi-empirical parametrization method to the analysis of a complex electronic system of the elements with partially filled 4f or 5f electron shells.

Our earlier experience in semi-empirical calculations for the above-mentioned elements was related to the americium, europium and praseodymium atoms [7–10]. On the basis of these studies, we observed that inclusion of higher configurations into the energy matrix and the extension of terms for the $4f^N$-core systematically improved the agreement between the calculated and experimental energy level values. A large amount of new experimental data of the hyperfine structure of the terbium atom, recently published by our experimental group [11–13], directs once again, our interest in the research of the rare-earth spectra. In ref. [13], recently published (2017), a parametric study of the fine structure (fs) and of the hyperfine structure (hfs) for even-parity configurations of atomic terbium (Tb I) was presented. We performed semi-empirical calculations on the basis of 7 even-parity configurations: $4f^85d^3$, $4f^85d^26s$, $4f^85d6s^2$, $4f^96s6p$, $4f^96s7p$, $4f^96s8p$ and $4f^95d6p$. In that work, we restricted the $4f^8$-core to 13 terms

[a] e-mail: magdalena.elantkowska@put.poznan.pl

(^{7}F + ^{5}S + ^{5}P + ^{5}D1, 2, 3 + ^{5}F1, 2 + ^{5}G1, 2, 3 + ^{5}H1, 2) and the $4f^9$-core to 3 terms (^{6}P + ^{6}F + ^{6}H). The considered system included 707 states for J quantum number ranging from 1/2 to 21/2.

In 2001, Zhang *et al.* reported the experimental and theoretical studies of Dy III [14]. In theoretical calculations, by means of the Cowan-code package [15,16], the adopted set of $4f^{10}$, $4f^9$6p and $4f^9$5d, $4f^9$6s configurations represented a total of 3549 possible energy levels. The same approach was used for calculations in doubly ionized europium [17, 18]. The configurations considered in the calculations were $4f^7$, $4f^6$6p for the odd parity and $4f^6$5d, $4f^6$6s for the even parity. This model contained a total number of 5323 possible energy levels.

In the current work we resigned from the previously mentioned limitations and performed the calculations for the terbium atom in the full number of $4f^8$- and $4f^9$-core states. In this case, the system contained 74418 possible energy levels corresponding to J values ranging from 1/2 to 31/2. The maximum rank of a single submatrix, for $J = 9/2$, was 9936. Such huge energy matrix for the rare-earth element was not previously considered.

It is clear that such a problem requires high-performance computing (HPC), concerning both CPU (Central Processing Unit) speed and memory allocation. The obvious choice would seem the supercomputing centres, but due to the batch queueing mode they are not optimal for iterative calculations requiring continuous interaction with the user. Therefore we propose alternative methods, allowing to use one's own computer clusters, generally available in the scientific laboratories. Another possibility is to use the Microsoft Azure cloud computing.

The essential aim of this work is therefore to answer the following questions:

- What impact on the results of the semi-empirical calculations has a consideration of the complete set of nf^N-core states?
- Can such calculations be performed within an acceptable time without the use of high-power computers?

2 Computational procedures

The construction of the fine-structure energy matrix requires calculation of numerous integrals dependent on the angular coordinates and various radial integrals [1]. The angular-dependent coefficients can be exactly determined, which is not possible in the case of radial integrals. Therefore, the matrix elements of the Hamiltonian are considered as linear combinations of radial integrals $P(k)$, where the angular integrals $\alpha_{ij}(k)$ serve as the coefficients of expansions,

$$H_{ij} = \sum_k \alpha_{ij}(k) P(k), \tag{1}$$

where i and j denote all possible SL states for the considered configuration system, and k represents the summation over all parameters described the interactions of the first- and higher-order perturbation theory, predicted by quantum mechanics.

The matrix elements of all operators are diagonal in J quantum number, therefore the energy matrix can be divided into submatrices corresponding to possible values of J. The rank of each submatrix is determined by the number of states with the same value of the total angular momentum J. For each submatrix a secular determinant is constructed:

$$\begin{vmatrix} H_{11} - E_J & H_{12} & H_{13} & \dots & H_{1j} \\ H_{21} & H_{22} - E_J & \dots & \dots & H_{2j} \\ H_{31} & H_{32} & H_{33} - E_J & \dots & H_{3j} \\ \dots & \dots & \dots & \dots & \dots \\ H_{i1} & \dots & \dots & \dots & H_{ij} - E_J \end{vmatrix} = 0. \tag{2}$$

The above-mentioned determinant, after expansion, is a polynomial of degree i with unknown energy values E_J. Every root of the polynomial approximates one of the possible eigenvalues of the Hamiltonian. In an iterative fitting procedure of experimental and calculated energy values the radial parameters and the eigenfunctions amplitudes are determined.

The main problem is the optimization of diagonalization procedures in such a way that the computing time of a single iteration will be as short as possible.

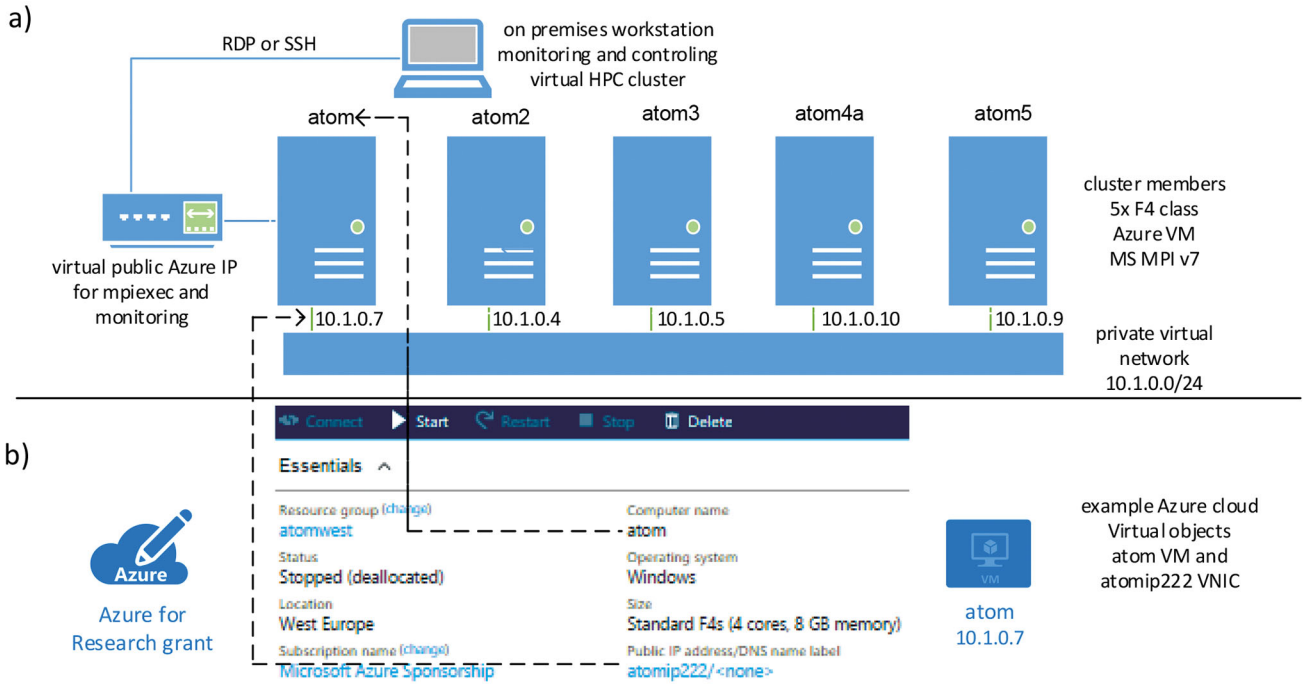

Fig. 1. HPC cluster for semi empirical terbium electronic structure calculations: (a) logical structure of Message Passing Interface (MPI) based cluster; (b) an example implementation with a set of Azure VMs. Please note that there are three possible deployment variants: Azure VMs, Azure Batch and local network with regular 4 core PCs. Designations used in the figure are only examples.

2.1 HPC calculations on Azure cloud

The underlying calculations were ported to Azure cloud, which resulted in a considerable performance boost. Indeed, the original calculations, implemented in a conventional sequential manner, required about ten hours per iteration, while it was reduced to less than three minutes when reprogrammed and launched on a cloud cluster. The achieved performance improvement was the result of individual H matrix blocks multithreaded diagonalization and, to an even greater degree, distribution over multiple nodes. The individual components of the block diagonal matrix were processed locally on Azure Virtual Machines (VMs) and only a small amount of data had to be exchanged among the cluster members. For now the local parallel processing is delegated to the multithreaded version of Intel Math Kernel Library (MKL), however in our future work we are going to develop our own tridiagonalization routines since MKL SSYEV procedure scales poorly on nodes with more than 4 CPU cores.

There are three possible variants considered for the implementation of the cluster (fig. 1). The most evident candidate, namely the Azure Batch [19], proved not suitable for our purposes since it requires data transfers of angular coefficients every time the process is initiated. The Azure File Storage shares did not result in sufficient improvement providing rather disappointing input-output (IO) rates. In contrast, the other two options, Azure VMs and a local cluster, performed well, the latter even when based on network file share. In the code listed below, we give the launching routine for static Azure cluster (cf. fig. 1 for nodes' names). The nodes are started asynchronously, reducing the time overhead (which was prohibitive in the Azure Batch service). Please note that it is essential to efficiently allocate and deallocate the cluster as the user is charged for VM time, not for the actual computation. We are going to publish a simple, "one click" open-source software application supporting easy configuration and control of the Azure VM-based HPC clusters:

```
string[] cluster = new string[]{"atom","atom2","atom3","atom4a","atom5" };
Task[] clusterT = new Task[cluster.Length];
ComputeManagementClient client=new ComputeManagementClient(token);
for (int i = 0; i < cluster.Length; i++)
clusterT[i] = client.VirtualMachines.StartAsync("atomwest", cluster[i]);
Task.WaitAll(clusterT);
```

2.2 Coordination of distributed tasks

Our cloud-oriented approach is based on two fundamental ideas, that enable efficient distribution of the workload while incurring limited communication and synchronization overhead. First, let us observe the H matrix is block diagonal (a very common case in quantum physics) allowing parallel processing of its components. Second, the semi-empirical tuning of radial coefficient requires only relatively small amount of data in the input file, which we transfer to one designated node responsible for the data collection and calculation of new radial values. Evidently (see sect. 2), the H matrix is a linear combination of radial and angular factors, thus the Jacobian involved in the radial calculation can be easily reconstructed at the mentioned "main" node. Simply put, member nodes transfer partial Jacobians and block until the main node returns new radial coefficients. Technically an MPI_Barrier is used for cluster coordination. This scheme can be considered an application of well-known multiway *rendez-vous* design pattern, whose two-way variant is present in ADA programming language. Disappointing performance of ssyev routine on nodes with 8 or more CPU cores made the efficient workload distribution a key performance factor in our project.

3 Results

The results of fs analysis are presented in table 1. The first two columns list the values of the experimental and calculated level energies. The energy and g_J values are taken from the NIST Atomic Spectra Database [20], whose primary source is the monograph by Martin *et al.* [21]. The fine-structure least-squares fit, using all 99 known experimental even-parity energy levels and 26 fitted parameters, resulted in a mean error for the energy level values of $\sigma(E) = 37\,\mathrm{cm}^{-1}$. The following four columns of table 1 contain the strongest and second strongest fine-structure components, as well as the corresponding percentages. Experimental g_j-Landé factors are known for 66 energy levels. In most cases, the discrepancies are observed in the third or the second decimal position (27 and 36 values, respectively), confirming the good quality of the obtained wave functions. In columns 7 and 8 of table 1 the calculated g_J values are compared with the experimental ones.

A comparison of current results with those published earlier [13] leads to the following conclusions. First, significantly better compliance of the calculated and the experimental energy values in the region up to $17000\,\mathrm{cm}^{-1}$ is noticeable. This is also confirmed by the much smaller root mean square value. Secondly, much more reliable description of the levels above $17000\,\mathrm{cm}^{-1}$ was achieved. In this energy range, our previous results [13], due to the applied limitations, indicated that the positions of the $4f^9 6s6p$ configuration states were not calculated correctly.

However, the final confirmation of the levels designations will be possible after the performing of the hyperfine-structure parametrization in the same, complete basis states. This requires the optimization and the adaptation of hyperfine-structure computational procedures for such a huge matrices. Encouraging results obtained in this work motivate us to undertake these tasks.

4 Conclusions

The preliminary results of fine-structure calculations indicate the need for considering the complete set of $4f^N$-core states. The comparison with the analysis, recently published [13], showed that the truncation of the number of $4f^8$ and $4f^9$ states affected even the energy levels in the region of several thousands cm^{-1}. Therefore, in our opinion, a reanalysis of the structure of rare-earth elements, conducted without any truncations, is highly recommended.

The way to achieve this purpose is the development of novelty kind of computational procedures optimization. Indeed, the MPI-based distribution and multithreaded diagonalization resulted in a 200 times performance boost over the original version, which enabled efficient execution of multiple session required to obtain desired radial coefficient accuracy. In our future work, we are going to investigate chances of overcoming the current memory bandwidth woes (*i.e.* the disappointing SSYEV performance on multicore CPU). We are also going to publish a user-friendly configuration assistant, facilitating streamlined configuration of Azure VM based HPC cluster, an attractive offer for the research community.

This work was performed in the framework of Microsoft Azure for Research grant awarded to Andrzej Sikorski. This work was partially supported by the Research Projects of the Polish Ministry of Sciences and Higher Education: 06/65/DSPB/0516 (ME) and 04/45/DSPB/0148 (JR and JD).

Table 1. Comparison of the experimental and calculated energy values [cm^{-1}] for Tb I.

E_{exp}	E_{calc}	ΔE	%	Main comp.	%	Sec. comp.	$g_{J\,calc}$	$g_{J\,exp}$	Δg_J
$J = 1/2$									
4018.210	4101	−83	87.4	$4f^8(^7F)5d6s^2\ ^8G$	2.9	$4f^8(^5D)5d6s^2\ ^6F$	−1.157	−1.191	−0.034
6259.090	6175	84	86.4	$4f^8(^7F)5d6s^2\ ^8F$	2.8	$4f^8(^5D)5d6s^2\ ^6D$	3.808	3.840	0.032
	11212		81.1	$4f^8(^7F)5d^26s\ ^{10}G$	8.6	$4f^8(^7F)5d^26s\ ^{10}G$	4.372		
	11243		81.6	$4f^8(^7F)5d6s^2\ ^6F$	3.5	$4f^8(^7F)5d^26s\ ^{10}G$	−0.370		
	13501		81.1	$4f^8(^7F)5d6s^2\ ^6D$	2.7	$4f^8(^7F)5d^26s\ ^6D$	3.242		
	14787		78.9	$4f^8(^7F)5d^26s\ ^{10}H$	7.3	$4f^8(^7F)5d^26s\ ^8G$	−1.790		
	15007		48.6	$4f^8(^7F)5d^26s\ ^8G$	18.5	$4f^8(^7F)5d^26s\ ^8G$	−1.215		
	16931		61.4	$4f^8(^7F)5d^26s\ ^8F$	18.1	$4f^8(^7F)5d^26s\ ^8F$	3.737		
	20024		82.4	$4f^8(^7F)5d^26s\ ^{10}G$	9.3	$4f^8(^7F)5d^26s\ ^{10}G$	4.594		
$J = 3/2$									
3705.820	3761	−55	80.1	$4f^8(^7F)5d6s^2\ ^8G$	8.6	$4f^8(^7F)5d6s^2\ ^8F$	1.045	1.022	−0.023
5483.980	5481	3	42.4	$4f^8(^7F)5d6s^2\ ^8F$	40.1	$4f^8(^7F)5d6s^2\ ^8D$	2.247	2.320	0.073
6849.720	6887	−37	48.8	$4f^8(^7F)5d6s^2\ ^8D$	37.5	$4f^8(^7F)5d6s^2\ ^8F$	2.385	2.335	−0.050
8336.310	8350	−14	83.5	$4f^8(^7F)5d6s^2\ ^8H$	4.4	$4f^8(^7F)5d6s^2\ ^6G$	−0.345	−0.360	−0.015
	10765		76.3	$4f^8(^7F)5d6s^2\ ^6F$	5.1	$4f^8(^7F)5d6s^2\ ^6G$	1.045		
10920.180	10899	21	77.4	$4f^8(^7F)5d^26s\ ^{10}G$	8.0	$4f^8(^7F)5d^26s\ ^{10}G$	2.150	2.145	−0.005
	12044		72.4	$4f^8(^7F)5d6s^2\ ^6G$	4.9	$4f^8(^7F)5d6s^2\ ^8H$	0.094		
	13049		72.0	$4f^8(^7F)5d6s^2\ ^6D$	6.0	$4f^8(^7F)5d6s^2\ ^6P$	1.844		
	13411		79.0	$4f^8(^7F)5d^26s\ ^{10}F$	7.9	$4f^8(^7F)5d^26s\ ^{10}F$	3.081		
	14555		32.6	$4f^8(^7F)5d^26s\ ^8G$	23.8	$4f^8(^7F)5d^26s\ ^{10}H$	0.937		
	14702		55.1	$4f^8(^7F)5d^26s\ ^{10}H$	16.6	$4f^8(^7F)5d^26s\ ^8G$	0.764		
	15388		78.9	$4f^8(^7F)5d6s^2\ ^6P$	5.8	$4f^8(^7F)5d6s^2\ ^6D$	2.332		
	15679		80.7	$4f^8(^7F)5d^26s\ ^{10}I$	11.1	$4f^8(^7F)5d^26s\ ^{10}H$	−0.577		
	16704		48.5	$4f^8(^7F)5d^26s\ ^8F$	14.1	$4f^8(^7F)5d^26s\ ^8F$	1.913		
	17936		73.9	$4f^8(^7F)5d^26s\ ^8H$	13.1	$4f^8(^7F)5d^26s\ ^8H$	−0.316		
	19285		64.3	$4f^8(^7F)5d^26s\ ^8D$	11.2	$4f^8(^7F)5d^26s\ ^8D$	2.662		
	19840		81.1	$4f^8(^7F)5d^26s\ ^{10}G$	9.3	$4f^8(^7F)5d^26s\ ^{10}G$	2.111		
	20480		32.2	$4f^8(^7F)5d^26s\ ^6F$	16.4	$4f^8(^7F)5d^26s\ ^6D$	1.137		
$J = 5/2$									
3174.575	3190	−15	67.4	$4f^8(^7F)5d6s^2\ ^8G$	17.8	$4f^8(^7F)5d6s^2\ ^8F$	1.374	1.355	−0.019
4695.505	4708	−13	48.6	$4f^8(^7F)5d6s^2\ ^8D$	22.7	$4f^8(^7F)5d6s^2\ ^8F$	1.803	1.831	0.028
6801.190	6807	−6	47.3	$4f^8(^7F)5d6s^2\ ^8F$	33.6	$4f^8(^7F)5d6s^2\ ^8D$	1.811	1.800	−0.011
8130.680	8131	−1	80.9	$4f^8(^7F)5d6s^2\ ^8H$	5.1	$4f^8(^7F)5d6s^2\ ^6G$	0.714	0.705	−0.009
10030.350	10037	−6	70.4	$4f^8(^7F)5d6s^2\ ^6F$	7.9	$4f^8(^7F)5d6s^2\ ^6G$	1.297	1.305	0.008
10456.670	10424	32	69.8	$4f^8(^7F)5d^26s\ ^{10}G$	11.6	$4f^8(^7F)5d^26s\ ^{10}F$	1.803	1.800	−0.003
	11577		63.1	$4f^8(^7F)5d6s^2\ ^6G$	7.7	$4f^8(^7F)5d6s^2\ ^6D$	0.953		
	11892		81.8	$4f^8(^7F)5d6s^2\ ^8P$	3.5	$4f^8(^7F)5d6s^2\ ^8D$	2.244		
12296.45	12262	35	52.1	$4f^8(^7F)5d6s^2\ ^6D$	16.0	$4f^8(^7F)5d6s^2\ ^6P$	1.605		
	13076		62.1	$4f^8(^7F)5d^26s\ ^{10}F$	10.1	$4f^8(^7F)5d^26s\ ^{10}D$	2.153		
	13211		82.0	$4f^8(^7F)5d6s^2\ ^6H$	3.6	$4f^8(^5D)5d6s^2\ ^4G$	0.330		
	14029		39.5	$4f^8(^7F)5d^26s\ ^8G$	18.3	$4f^8(^7F)5d^26s\ ^8G$	1.352		
	14356		65.4	$4f^8(^7F)5d6s^2\ ^6P$	15.6	$4f^8(^7F)5d6s^2\ ^6D$	1.826		
	14437		63.9	$4f^8(^7F)5d^26s\ ^{10}H$	20.1	$4f^8(^7F)5d^26s\ ^{10}I$	1.096		
	15683		70.1	$4f^8(^7F)5d^26s\ ^{10}I$	19.8	$4f^8(^7F)5d^26s\ ^{10}H$	0.679		

Table 1. Continued.

$E_{\rm exp}$	$E_{\rm calc}$	ΔE	%	Main comp.	%	Sec. comp.	$g_{J\,\rm calc}$	$g_{J\,\rm exp}$	Δg_J
	16000		23.3	$4f^8(^7F)5d^26s\ ^{10}D$	15.2	$4f^8(^7F)5d^26s\ ^8D$	2.047		
	16148		54.7	$4f^8(^7F)5d^26s\ ^{10}D$	11.3	$4f^8(^7F)5d^26s\ ^8F$	2.224		
	17449		27.8	$4f^8(^7F)5d^26s\ ^8P$	21.3	$4f^8(^7F)5d^26s\ ^8H$	1.591		
	17736		35.8	$4f^8(^7F)5d^26s\ ^8H$	10.6	$4f^8(^7F)5d^26s\ ^8P$	1.053		
	18135		87.8	$4f^8(^7F)5d^26s\ ^{10}D$	2.7	$4f^8(^5D)5d^26s\ ^8P$	2.537		
	18749		20.0	$4f^8(^5D)5d6s^2\ ^6P$	15.5	$4f^8(^5D)5d6s^2\ ^6P$	1.763		
	18782		60.3	$4f^8(^7F)5d^26s\ ^8I$	12.1	$4f^8(^7F)5d^26s\ ^8H$	0.158		
	19515		22.6	$4f^8(^7F)5d^26s\ ^6F$	18.0	$4f^8(^7F)5d^26s\ ^6D$	1.464		
	19546		70.2	$4f^8(^7F)5d^26s\ ^{10}G$	8.4	$4f^8(^7F)5d^26s\ ^{10}G$	1.724		
	20166		37.1	$4f^8(^7F)5d^26s\ ^8D$	15.7	$4f^8(^7F)5d^26s\ ^8P$	2.044		
	20479		29.1	$4f^8(^7F)5d^26s\ ^6G$	17.3	$4f^8(^7F)5d^26s\ ^6P$	1.263		
$J = 7/2$									
2419.480	2400	20	51.0	$4f^8(^7F)5d6s^2\ ^8G$	26.1	$4f^8(^7F)5d6s^2\ ^8F$	1.488	1.477	−0.012
3819.850	3839	−20	47.4	$4f^8(^7F)5d6s^2\ ^8D$	28.7	$4f^8(^7F)5d6s^2\ ^8G$	1.630	1.642	0.012
6488.280	6464	24	51.7	$4f^8(^7F)5d6s^2\ ^8F$	21.6	$4f^8(^7F)5d6s^2\ ^8D$	1.640	1.635	−0.005
7839.850	7823	17	76.6	$4f^8(^7F)5d6s^2\ ^8H$	6.2	$4f^8(^7F)5d6s^2\ ^6G$	1.070	1.050	−0.020
8994.660	9015	−21	62.0	$4f^8(^7F)5d6s^2\ ^6F$	12.8	$4f^8(^7F)5d6s^2\ ^6D$	1.404	1.414	0.010
9867.650	9830	38	61.5	$4f^8(^7F)5d^26s\ ^{10}G$	16.8	$4f^8(^7F)5d^26s\ ^{10}F$	1.684	1.680	−0.004
10324.740	10314	10	74.0	$4f^8(^7F)5d6s^2\ ^8P$	8.4	$4f^8(^7F)5d6s^2\ ^8D$	1.894	1.916	0.022
	10558		27.4	$4f^8(^7F)5d6s^2\ ^6D$	26.0	$4f^8(^7F)5d6s^2\ ^6P$	1.470		
11107.07	11120	−13	39.7	$4f^8(^7F)5d6s^2\ ^6G$	17.4	$4f^8(^7F)5d6s^2\ ^6F$	1.298		
12250.99	12290	−39	26.6	$4f^8(^7F)5d^26s\ ^{10}F$	22.5	$4f^8(^7F)5d^26s\ ^{10}D$	1.936		
12645.32	12658	−13	72.6	$4f^8(^7F)5d6s^2\ ^6H$	3.6	$4f^8(^7F)5d6s^2\ ^8H$	0.919		
12714.050	12784	−70	35.2	$4f^8(^7F)5d6s^2\ ^6D$	33.2	$4f^8(^7F)5d6s^2\ ^6P$	1.590		
13277.23	13288	−10	27.2	$4f^8(^7F)5d^26s\ ^8G$	12.9	$4f^8(^7F)5d^26s\ ^8G$	1.528		
13729.12	13732	−3	31.6	$4f^8(^7F)5d^26s\ ^{10}P$	19.4	$4f^8(^7F)5d^26s\ ^{10}F$	1.861		
	14150		36.8	$4f^8(^7F)5d^26s\ ^{10}H$	18.5	$4f^8(^7F)5d^26s\ ^{10}I$	1.435		
	14346		21.6	$4f^8(^7F)5d^26s\ ^{10}P$	12.1	$4f^8(^7F)5d^26s\ ^8S$	1.812		
	15641		61.8	$4f^8(^7F)5d^26s\ ^{10}I$	25.8	$4f^8(^7F)5d^26s\ ^{10}H$	1.070		
	16070		25.1	$4f^8(^7F)5d^26s\ ^8F$	11.4	$4f^8(^7F)5d^26s\ ^8D$	1.603		
	16935		41.9	$4f^8(^7F)5d^26s\ ^{10}D$	23.7	$4f^8(^7F)5d^26s\ ^{10}D$	2.072		
	17287		52.7	$4f^8(^7F)5d^26s\ ^{10}D$	12.5	$4f^8(^7F)5d^26s\ ^{10}D$	1.851		
	17315		33.3	$4f^8(^7F)5d^26s\ ^8H$	13.9	$4f^8(^7F)5d^26s\ ^8I$	1.262		
	18343		11.8	$4f^8(^5D)5d6s^2\ ^6D$	8.4	$4f^8(^5D)5d6s^2\ ^6D$	1.640		
	18432		11.4	$4f^8(^5D)5d6s^2\ ^6D$	8.9	$4f^8(^7F)5d^26s\ ^8P$	1.639		
	18719		43.5	$4f^8(^7F)5d^26s\ ^8I$	16.6	$4f^8(^7F)5d^26s\ ^8H$	0.877		
	18815		22.8	$4f^8(^7F)5d^26s\ ^6F$	14.6	$4f^8(^7F)5d^26s\ ^6D$	1.384		
	19132		75.4	$4f^8(^7F)5d^26s\ ^{10}G$	9.1	$4f^8(^7F)5d^26s\ ^{10}G$	1.638		
	19601		41.8	$4f^8(^7F)5d^26s\ ^8D$	17.0	$4f^8(^7F)5d^26s\ ^8D$	1.718		
	19928		19.9	$4f^8(^7F)5d^26s\ ^6G$	12.1	$4f^8(^7F)5d^26s\ ^8D$	1.398		
	20184		14.3	$4f^8(^7F)5d^26s\ ^6P$	10.6	$4f^8(^7F)5d^26s\ ^6D$	1.497		
	20849		13.4	$4f^8(^7F)5d^26s\ ^8G$	9.0	$4f^8(^7F)5d^26s\ ^8F$	1.567		
$J = 9/2$									
1371.045	1332	39	31.5	$4f^8(^7F)5d6s^2\ ^8G$	29.5	$4f^8(^7F)5d6s^2\ ^8F$	1.545	1.541	−0.004
2840.170	2864	−23	43.9	$4f^8(^7F)5d6s^2\ ^8G$	36.1	$4f^8(^7F)5d6s^2\ ^8D$	1.541	1.544	0.002

Table 1. Continued.

$E_{\rm exp}$	$E_{\rm calc}$	ΔE	%	Main comp.	%	Sec. comp.	$g_{J\,\rm calc}$	$g_{J\ \rm exp}$	Δg_J
5829.860	5780	50	50.7	$4f^8(^7F)5d6s^2\ ^8F$	14.5	$4f^8(^7F)5d6s^2\ ^8P$	1.578	1.580	0.002
7441.030	7398	43	66.4	$4f^8(^7F)5d6s^2\ ^8H$	9.5	$4f^8(^7F)5d6s^2\ ^6G$	1.247	1.240	−0.007
7824.190	7874	−49	60.0	$4f^8(^7F)5d6s^2\ ^6F$	11.1	$4f^8(^7F)5d6s^2\ ^6D$	1.413	1.433	0.020
8097.875	8103	−5	61.1	$4f^8(^7F)5d6s^2\ ^8P$	19.5	$4f^8(^7F)5d6s^2\ ^8D$	1.727	1.750	0.023
9145.230	9118	27	46.3	$4f^8(^7F)5d^26s\ ^{10}G$	19.6	$4f^8(^7F)5d^26s\ ^{10}F$	1.673	1.670	−0.003
9897.730	9886	12	26.5	$4f^8(^7F)5d^26s\ ^{10}S$	19.8	$4f^8(^7F)5d6s^2\ ^6G$	1.668	1.810	0.142
9986.73	9934	53	29.7	$4f^8(^7F)5d6s^2\ ^6G$	18.8	$4f^8(^7F)5d^26s\ ^{10}S$	1.567		
10680.17	10662	19	49.1	$4f^8(^7F)5d6s^2\ ^6D$	19.6	$4f^8(^7F)5d6s^2\ ^6F$	1.474		
11956.255	11943	14	72.6	$4f^8(^7F)5d6s^2\ ^6H$	6.8	$4f^8(^7F)5d6s^2\ ^8H$	1.104		
12228.28	12270	−42	36.8	$4f^8(^7F)5d^26s\ ^{10}F$	15.5	$4f^8(^7F)5d^26s\ ^{10}D$	1.727		
12776.31	12790	−13	29.0	$4f^8(^7F)5d^26s\ ^8G$	15.8	$4f^8(^7F)5d^26s\ ^8F$	1.468		
13751.41	13785	−33	46.1	$4f^8(^7F)5d^26s\ ^{10}H$	28.3	$4f^8(^7F)5d^26s\ ^{10}I$	1.364		
	14709		25.7	$4f^8(^7F)5d^26s\ ^{10}P$	22.5	$4f^8(^7F)5d^26s\ ^{10}S$	1.850		
	15141		20.5	$4f^8(^7F)5d^26s\ ^8D$	14.1	$4f^8(^7F)5d^26s\ ^8P$	1.582		
	15537		54.0	$4f^8(^7F)5d^26s\ ^{10}I$	29.9	$4f^8(^7F)5d^26s\ ^{10}H$	1.244		
	16025		85.4	$4f^8(^7F)5d^26s\ ^{10}D$	3.7	$4f^8(^7F)5d^26s\ ^8D$	1.854		
	16715		30.6	$4f^8(^7F)5d^26s\ ^8H$	13.5	$4f^8(^7F)5d^26s\ ^8P$	1.333		
	17314		18.5	$4f^8(^7F)5d^26s\ ^8P$	16.2	$4f^8(^7F)5d^26s\ ^8F$	1.509		
	17631		47.0	$4f^8(^7F)5d^26s\ ^{10}D$	28.4	$4f^8(^7F)5d^26s\ ^{10}P$	1.876		
	18251		21.9	$4f^8(^5D)5d6s^2\ ^6F$	18.1	$4f^8(^5D)5d6s^2\ ^6D$	1.459		
	18307		47.3	$4f^8(^7F)5d^26s\ ^8D$	20.0	$4f^8(^7F)5d^26s\ ^8D$	1.661		
	18470		20.8	$4f^8(^7F)5d^26s\ ^8I$	13.1	$4f^8(^7F)5d^26s\ ^6G$	1.212		
	18611		46.2	$4f^8(^7F)5d^26s\ ^{10}G$	6.6	$4f^8(^7F)5d^26s\ ^{10}G$	1.474		
	18643		25.3	$4f^8(^7F)5d^26s\ ^{10}G$	17.5	$4f^8(^7F)5d^26s\ ^8I$	1.315		
	19274		12.0	$4f^8(^7F)5d^26s\ ^8P$	8.1	$4f^8(^7F)5d^26s\ ^6H$	1.468		
	19632		26.8	$4f^8(^7F)5d^3\ ^{10}D$	16.6	$4f^8(^7F)5d^3\ ^{10}P$	1.740		
	19858		13.0	$4f^8(^7F)5d^26s\ ^8P$	11.5	$4f^8(^7F)5d^3\ ^{10}D$	1.616		
	20199		17.8	$4f^8(^7F)5d^26s\ ^8D$	14.6	$4f^8(^7F)5d^26s\ ^8P$	1.605		
	20563		12.5	$4f^8(^7F)5d^26s\ ^6H$	11.6	$4f^8(^7F)5d^26s\ ^8G$	1.370		
	20583		24.6	$4f^8(^7F)5d^26s\ ^8D$	15.3	$4f^8(^7F)5d^26s\ ^8P$	1.636		
$J = 11/2$									
509.845	476	34	32.6	$4f^8(^7F)5d6s^2\ ^8G$	31.1	$4f^8(^7F)5d6s^2\ ^8F$	1.519	1.517	−0.002
2310.090	2336	−26	45.7	$4f^8(^7F)5d6s^2\ ^8D$	40.5	$4f^8(^7F)5d6s^2\ ^8G$	1.529	1.530	0.002
5353.370	5334	19	50.4	$4f^8(^7F)5d6s^2\ ^8F$	21.7	$4f^8(^7F)5d6s^2\ ^8D$	1.534	1.545	0.011
6674.155	6700	−26	51.2	$4f^8(^7F)5d6s^2\ ^6F$	18.3	$4f^8(^7F)5d6s^2\ ^6G$	1.415	1.320	−0.095
6988.820	6996	−7	60.8	$4f^8(^7F)5d6s^2\ ^8H$	18.0	$4f^8(^7F)5d6s^2\ ^6F$	1.330	1.315	−0.015
8646.210	8623	24	53.2	$4f^8(^7F)5d^26s\ ^{10}G$	21.3	$4f^8(^7F)5d^26s\ ^{10}F$	1.586	1.600	0.014
8932.120	8905	27	54.0	$4f^8(^7F)5d6s^2\ ^6G$	14.8	$4f^8(^7F)5d6s^2\ ^6F$	1.347	1.470	0.123
10997.850	10967	31	70.9	$4f^8(^7F)5d6s^2\ ^6H$	9.9	$4f^8(^7F)5d6s^2\ ^8H$	1.224	1.210	−0.014
11260.41	11303	−43	25.3	$4f^8(^7F)5d^26s\ ^{10}D$	20.0	$4f^8(^7F)5d^26s\ ^{10}P$	1.669	1.680	0.011
12453.14	12471	−18	28.3	$4f^8(^7F)5d^26s\ ^8G$	15.7	$4f^8(^7F)5d^26s\ ^8G$	1.474		
13071.30	13082	−11	28.4	$4f^8(^7F)5d^26s\ ^{10}H$	27.6	$4f^8(^7F)5d^26s\ ^{10}P$	1.564		
13666.46	13678	−11	19.9	$4f^8(^7F)5d^26s\ ^{10}I$	18.7	$4f^8(^7F)5d^26s\ ^{10}P$	1.538		
	14597		78.4	$4f^8(^7F)5d^26s\ ^{10}D$	5.7	$4f^8(^7F)5d^26s\ ^{10}F$	1.734		
	15249		21.9	$4f^8(^7F)5d^26s\ ^8F$	12.2	$4f^8(^7F)5d^26s\ ^8H$	1.498		

Table 1. Continued.

E_{exp}	E_{calc}	ΔE	%	Main comp.	%	Sec. comp.	$g_{J\,calc}$	$g_{J\,exp}$	Δg_J
	15335		49.4	$4f^8(^7F)5d^26s\ ^{10}I$	31.8	$4f^8(^7F)5d^26s\ ^{10}H$	1.323		
	16439		22.0	$4f^8(^7F)5d^26s\ ^{8}H$	14.5	$4f^8(^7F)5d^26s\ ^{8}I$	1.367		
	16920		27.9	$4f^8(^7F)5d^26s\ ^{8}D$	18.5	$4f^8(^7F)5d^26s\ ^{8}D$	1.553		
	17031		54.4	$4f^8(^7F)5d^26s\ ^{10}D$	21.1	$4f^8(^7F)5d^26s\ ^{10}P$	1.744		
	17988		65.4	$4f^8(^7F)5d^26s\ ^{10}G$	9.1	$4f^8(^7F)5d^26s\ ^{10}G$	1.541		
	18145		18.5	$4f^8(^7F)5d^26s\ ^{8}I$	18.3	$4f^8(^7F)5d^26s\ ^{6}H$	1.260		
	18337		21.8	$4f^8(^7F)5d^26s\ ^{8}H$	17.9	$4f^8(^7F)5d^26s\ ^{8}I$	1.256		
	18793		36.3	$4f^9(^6H)6s6p\ ^{4}G$	9.0	$4f^9(^6H)6s6p\ ^{6}G$	1.325		
	18922		24.9	$4f^8(^7F)5d^26s\ ^{8}D$	8.9	$4f^8(^7F)5d^26s\ ^{6}F$	1.474		
	19235		14.0	$4f^8(^7F)5d^26s\ ^{8}D$	10.9	$4f^8(^7F)5d^26s\ ^{8}F$	1.455		
	19361		22.5	$4f^8(^5D)5d6s^2\ ^{6}F$	18.3	$4f^8(^5D)5d6s^2\ ^{6}F$	1.413		
	19463		42.5	$4f^8(^7F)5d^3\ ^{10}D$	25.3	$4f^8(^7F)5d^3\ ^{10}F$	1.714		
	19736		9.1	$4f^8(^5D)5d6s^2\ ^{6}F$	7.5	$4f^8(^5D)5d6s^2\ ^{6}F$	1.364		
	19780		8.5	$4f^9(^6H)6s6p\ ^{8}H$	7.9	$4f^8(^7F)5d^26s\ ^{8}G$	1.377		
	20043		15.4	$4f^8(^7F)5d^26s\ ^{8}F$	8.4	$4f^8(^7F)5d^26s\ ^{8}D$	1.465		
	20401		18.5	$4f^8(^7F)5d^26s\ ^{8}D$	10.9	$4f^8(^7F)5d^26s\ ^{6}G$	1.384		
	20558		35.8	$4f^8(^7F)5d^26s\ ^{8}G$	8.2	$4f^8(^7F)5d^26s\ ^{6}G$	1.416		
	20924		19.5	$4f^9(^6H)6s6p\ ^{6}G$	11.8	$4f^9(^6H)6s6p\ ^{8}H$	1.310		
	21069		17.6	$4f^8(^7F)5d^26s\ ^{6}I$	11.8	$4f^8(^7F)5d^26s\ ^{8}D$	1.268		
	21159		9.0	$4f^8(^7F)5d^26s\ ^{8}H$	8.9	$4f^8(^7F)5d^26s\ ^{6}H$	1.354		
	21523		7.6	$4f^8(^7F)5d^26s\ ^{8}D$	7.1	$4f^8(^7F)5d^26s\ ^{8}H$	1.404		
	21717		17.8	$4f^9(^6H)6s6p\ ^{8}G$	8.4	$4f^9(^6H)6s6p\ ^{4}H$	1.240		
	21854		17.2	$4f^9(^6H)6s6p\ ^{8}I$	14.0	$4f^9(^6H)6s6p\ ^{6}I$	1.182		
	21984		14.5	$4f^8(^7F)5d^26s\ ^{10}F$	6.3	$4f^8(^7F)5d^26s\ ^{6}F$	1.357		
	22176		18.0	$4f^8(^7F)5d^26s\ ^{10}F$	4.8	$4f^8(^7F)5d^26s\ ^{6}I$	1.434		
	22217		23.0	$4f^8(^7F)5d^3\ ^{10}P$	21.2	$4f^8(^7F)5d^3\ ^{10}F$	1.649		
	22231		11.5	$4f^9(^6H)6s6p\ ^{4}G$	10.1	$4f^8(^7F)5d^26s\ ^{10}F$	1.355		
	22442		15.4	$4f^8(^7F)5d^26s\ ^{10}F$	9.3	$4f^8(^7F)5d^26s\ ^{8}I$	1.404		
	22561		13.3	$4f^8(^7F)5d^26s\ ^{6}F$	10.7	$4f^8(^7F)5d^26s\ ^{6}G$	1.348		
	22742		31.2	$4f^8(^7F)5d^26s\ ^{4}H$	10.2	$4f^8(^7F)5d^26s\ ^{4}G$	1.243		
	22797		28.6	$4f^8(^7F)5d^26s\ ^{8}D$	17.9	$4f^8(^7F)5d^26s\ ^{8}D$	1.526		
	23192		10.0	$4f^8(^7F)5d^26s\ ^{6}F$	6.7	$4f^8(^7F)5d^26s\ ^{6}F$	1.354		
	23242		7.4	$4f^8(^7F)5d^26s\ ^{8}G$	6.4	$4f^8(^7F)5d^26s\ ^{6}G$	1.315		
	23291		8.7	$4f^9(^6F)6s6p\ ^{8}D$	5.3	$4f^9(^6H)6s6p\ ^{8}H$	1.311		
	23357		19.7	$4f^9(^6F)6s6p\ ^{8}D$	7.7	$4f^9(^6F)6s6p\ ^{8}F$	1.417		
	23530		11.2	$4f^8(^7F)5d^26s\ ^{4}G$	9.1	$4f^8(^7F)5d^26s\ ^{8}G$	1.344		
	23625		13.4	$4f^9(^6H)6s6p\ ^{8}G$	10.6	$4f^9(^6H)6s6p\ ^{8}H$	1.300		
	23722		13.9	$4f^9(^6F)6s6p\ ^{8}D$	13.7	$4f^9(^6H)6s6p\ ^{4}H$	1.321		
	23806		40.5	$4f^8(^7F)5d^3\ ^{10}H$	28.1	$4f^8(^7F)5d^3\ ^{10}I$	1.400		
	23864		7.5	$4f^9(^6H)6s6p\ ^{8}I$	6.6	$4f^8(^7F)5d^26s\ ^{8}I$	1.309		
	24221		8.9	$4f^8(^7F)5d^26s\ ^{8}F$	7.2	$4f^8(^7F)5d^26s\ ^{8}G$	1.341		
	24364		8.1	$4f^8(^7F)5d^26s\ ^{8}G$	7.8	$4f^8(^7F)5d^26s\ ^{4}G$	1.305		
	24551		9.6	$4f^8(^7F)5d^26s\ ^{8}H$	8.7	$4f^8(^7F)5d^26s\ ^{8}H$	1.408		
	24579		13.2	$4f^8(^7F)5d^26s\ ^{4}G$	13.1	$4f^8(^7F)5d^26s\ ^{8}F$	1.405		
	24641		12.3	$4f^9(^6F)6s6p\ ^{8}G$	7.1	$4f^9(^6F)6s6p\ ^{6}G$	1.309		

Table 1. Continued.

$E_{\rm exp}$	$E_{\rm calc}$	ΔE	%	Main comp.	%	Sec. comp.	$g_{J\,\rm calc}$	$g_{J\,\rm exp}$	Δg_J
	24670		7.1	$4f^8(^5G)5d6s^2\ ^6F$	6.9	$4f^8(^5G)5d6s^2\ ^6F$	1.320		
	25012		42.7	$4f^8(^7F)5d^3\ ^{10}P$	26.4	$4f^8(^7F)5d^3\ ^{10}D$	1.698		
	25074		11.2	$4f^8(^7F)5d^26s\ ^6I$	6.7	$4f^8(^7F)5d^26s\ ^8F$	1.289		
	25160		11.6	$4f^9(^6F)6s6p\ ^4G$	6.9	$4f^8(^7F)5d^26s\ ^4I$	1.268		
	25233		16.2	$4f^9(^6F)6s6p\ ^4G$	12.3	$4f^9(^6F)6s6p\ ^6F$	1.277		
	25303		12.5	$4f^8(^7F)5d^26s\ ^8D$	7.2	$4f^9(^6H)6s6p\ ^6G$	1.397		
	25381		30.3	$4f^8(^7F)5d^3\ ^{10}I$	9.6	$4f^8(^7F)5d^3\ ^{10}G$	1.367		
	25413		18.1	$4f^9(^6H)6s6p\ ^6G$	12.2	$4f^8(^7F)5d^3\ ^{10}I$	1.298		
	25579		23.9	$4f^8(^7F)5d^26s\ ^4I$	8.3	$4f^8(^7F)5d^26s\ ^8D$	1.229		
25637.87	25634	4	8.9	$4f^8(^7F)5d^26s\ ^8I$	7.3	$4f^8(^7F)5d^26s\ ^8H$	1.348	1.334	−0.014
	25797		37.8	$4f^8(^5L)5d6s^2\ ^6L$	4.7	$4f^8(^7F)5d^26s\ ^8F$	0.928		
	25842		13.6	$4f^8(^7F)5d^26s\ ^8F$	11.5	$4f^8(^5L)5d6s^2\ ^6L$	1.215		
	26109		8.9	$4f^8(^7F)5d^26s\ ^8G$	7.6	$4f^8(^7F)5d^26s\ ^6I$	1.342		
	26239		9.6	$4f^9(^6H)6s6p\ ^6I$	7.4	$4f^9(^6H)6s6p\ ^4I$	1.191		
	26308		8.6	$4f^8(^7F)5d^26s\ ^6H$	8.3	$4f^9(^6H)6s6p\ ^6I$	1.175		
26553.26	26506	47	10.9	$4f^9(^6F)6s6p\ ^6F$	10.1	$4f^8(^5D)5d6s^2\ ^6G$	1.334		
	26602		11.6	$4f^8(^7F)5d^26s\ ^8I$	10.5	$4f^9(^6F)6s6p\ ^6F$	1.266		
$J = 13/2$									
285.500	286	−1	59.2	$4f^8(^7F)5d6s^2\ ^8G$	25.1	$4f^8(^7F)5d6s^2\ ^8F$	1.466	1.464	−0.002
3719.705	3668	52	65.0	$4f^8(^7F)5d6s^2\ ^8F$	22.2	$4f^8(^7F)5d6s^2\ ^8G$	1.504	1.505	0.001
6351.750	6306	46	67.8	$4f^8(^7F)5d6s^2\ ^8H$	11.1	$4f^8(^7F)5d6s^2\ ^6G$	1.355	1.350	−0.005
7059.900	7039	21	63.2	$4f^8(^7F)5d6s^2\ ^6G$	11.4	$4f^8(^7F)5d6s^2\ ^6H$	1.370	1.380	0.010
8277.040	8266	11	56.4	$4f^8(^7F)5d^26s\ ^{10}G$	19.3	$4f^8(^7F)5d^26s\ ^{10}F$	1.555	1.570	0.015
9763.020	9757	6	70.4	$4f^8(^7F)5d6s^2\ ^6H$	12.7	$4f^8(^7F)5d6s^2\ ^8H$	1.297	1.300	0.003
11425.94	11417	9	31.5	$4f^8(^7F)5d^26s\ ^{10}F$	12.0	$4f^8(^7F)5d^26s\ ^{10}D$	1.569		
12475.74	12465	11	25.0	$4f^8(^7F)5d^26s\ ^8G$	15.8	$4f^8(^7F)5d^26s\ ^{10}D$	1.503		
12906.60	12858	48	42.3	$4f^8(^7F)5d^26s\ ^{10}D$	22.6	$4f^8(^7F)5d^26s\ ^{10}H$	1.544		
13116.48	13141	−25	24.8	$4f^8(^7F)5d^26s\ ^{10}D$	17.9	$4f^8(^7F)5d^26s\ ^{10}I$	1.525		
	15013		47.2	$4f^8(^7F)5d^26s\ ^{10}I$	27.0	$4f^8(^7F)5d^26s\ ^{10}H$	1.383		
	15193		22.9	$4f^8(^7F)5d^26s\ ^8F$	17.0	$4f^8(^7F)5d^26s\ ^{10}D$	1.489		
	15663		42.1	$4f^8(^7F)5d^26s\ ^{10}D$	14.6	$4f^8(^7F)5d^26s\ ^8H$	1.521		
	16322		14.8	$4f^9(^6H)6s6p\ ^4H$	13.9	$4f^9(^6H)6s6p\ ^6G$	1.370		
	16397		14.4	$4f^8(^7F)5d^26s\ ^8F$	8.8	$4f^8(^7F)5d^26s\ ^8I$	1.409		
	17262		64.2	$4f^8(^7F)5d^26s\ ^{10}G$	9.9	$4f^8(^7F)5d^26s\ ^{10}G$	1.530		
17875.98	17886	−10	32.6	$4f^8(^7F)5d^26s\ ^8I$	18.5	$4f^8(^7F)5d^26s\ ^8H$	1.288		
	17951		24.6	$4f^8(^7F)5d^26s\ ^6H$	11.2	$4f^8(^7F)5d^26s\ ^6G$	1.314		
	18434		31.1	$4f^9(^6H)6s6p\ ^4H$	26.1	$4f^9(^6H)6s6p\ ^6G$	1.315		
	18867		25.7	$4f^9(^6H)6s6p\ ^6G$	20.7	$4f^9(^6H)6s6p\ ^8H$	1.343		
	19156		18.4	$4f^8(^7F)5d^26s\ ^8G$	14.7	$4f^8(^7F)5d^26s\ ^8G$	1.420		
	19555		21.7	$4f^8(^7F)5d^26s\ ^6G$	6.8	$4f^8(^7F)5d^26s\ ^8F$	1.371		
	19666		32.0	$4f^8(^7F)5d^3\ ^{10}F$	22.7	$4f^8(^7F)5d^3\ ^{10}D$	1.568		
	19809		8.3	$4f^9(^6H)6s6p\ ^8G$	7.9	$4f^9(^6H)6s6p\ ^6I$	1.390		
	19831		37.2	$4f^8(^7F)5d^26s\ ^8G$	8.2	$4f^8(^7F)5d^26s\ ^8G$	1.444		
	20113		14.5	$4f^9(^6H)6s6p\ ^6I$	8.4	$4f^9(^6H)6s6p\ ^4I$	1.311		
	20379		27.2	$4f^8(^7F)5d^26s\ ^6I$	11.8	$4f^8(^7F)5d^26s\ ^6I$	1.239		

Table 1. Continued.

$E_{\rm exp}$	$E_{\rm calc}$	ΔE	%	Main comp.	%	Sec. comp.	$g_{J\,\rm calc}$	$g_{J\ \rm exp}$	Δg_J
	20858		23.0	$4f^8(^7F)5d^26s\ ^8F$	15.5	$4f^8(^7F)5d^26s\ ^{10}F$	1.465		
	21088		17.5	$4f^9(^6H)6s6p\ ^6G$	10.2	$4f^8(^5D)5d6s^2\ ^6G$	1.376		
	21163		18.4	$4f^8(^7F)5d^26s\ ^{10}F$	6.0	$4f^9(^6H)6s6p\ ^6G$	1.430		
	21358		26.8	$4f^8(^7F)5d^26s\ ^4H$	16.2	$4f^8(^7F)5d^26s\ ^6H$	1.296		
	21425		11.4	$4f^9(^6H)6s6p\ ^6H$	11.2	$4f^9(^6H)6s6p\ ^8I$	1.310		
	21610		11.1	$4f^9(^6H)6s6p\ ^6H$	8.6	$4f^9(^6H)6s6p\ ^8G$	1.312		
	21691		15.6	$4f^8(^7F)5d^26s\ ^{10}F$	9.4	$4f^8(^7F)5d^26s\ ^6G$	1.393		
	21713		9.4	$4f^8(^7F)5d^26s\ ^8G$	9.1	$4f^9(^6H)6s6p\ ^6H$	1.329		
	22100		17.9	$4f^8(^7F)5d^26s\ ^6H$	8.6	$4f^8(^7F)5d^26s\ ^6G$	1.290		
	22438		23.2	$4f^8(^7F)5d^3\ ^{10}D$	7.0	$4f^8(^7F)5d^26s\ ^8F$	1.513		
	22620		30.6	$4f^8(^7F)5d^3\ ^{10}D$	7.9	$4f^8(^7F)5d^3\ ^{10}F$	1.548		
	22733		13.6	$4f^8(^5D)5d6s^2\ ^6G$	13.3	$4f^9(^6H)6s6p\ ^6G$	1.346		
23043.43	23030	14	9.9	$4f^8(^7F)5d^26s\ ^6H$	9.2	$4f^8(^7F)5d^26s\ ^6G$	1.363	1.391	0.028
23112.35	23095	17	10.5	$4f^8(^7F)5d^26s\ ^8I$	7.4	$4f^8(^7F)5d^26s\ ^8F$	1.368		
	23235		34.4	$4f^8(^7F)5d^3\ ^{10}H$	22.9	$4f^8(^7F)5d^3\ ^{10}I$	1.448		
	23262		14.6	$4f^8(^7F)5d^26s\ ^8F$	8.1	$4f^8(^7F)5d^26s\ ^8G$	1.412		
	23308		12.3	$4f^9(^6H)6s6p\ ^4I$	12.1	$4f^9(^6H)6s6p\ ^8H$	1.286		
	23515		8.8	$4f^9(^6H)6s6p\ ^6G$	5.5	$4f^8(^5G)5d6s^2\ ^6H$	1.309		
	23872		15.5	$4f^9(^6F)6s6p\ ^8F$	13.2	$4f^9(^6F)6s6p\ ^8G$	1.420		
	23940		16.5	$4f^8(^7F)5d^26s\ ^8H$	10.2	$4f^8(^7F)5d^26s\ ^8H$	1.360		
	24060		16.8	$4f^8(^7F)5d^26s\ ^4I$	9.1	$4f^9(^6F)6s6p\ ^8F$	1.333		
	24379		15.9	$4f^8(^7F)5d^26s\ ^6I$	13.2	$4f^8(^7F)5d^26s\ ^6I$	1.270		
	24548		21.1	$4f^8(^7F)5d^26s\ ^4I$	6.8	$4f^8(^7F)5d^26s\ ^6G$	1.282		
	24868		24.6	$4f^9(^6H)6s6p\ ^6I$	17.6	$4f^9(^6H)6s6p\ ^8I$	1.212		
	24935		51.0	$4f^8(^7F)5d^3\ ^{10}I$	19.1	$4f^8(^7F)5d^3\ ^{10}G$	1.407		
	25125		13.2	$4f^8(^7F)5d^26s\ ^8H$	9.2	$4f^8(^7F)5d^26s\ ^8H$	1.329		
25373.85	25286	88	11.9	$4f^8(^7F)5d^26s\ ^8I$	11.6	$4f^8(^7F)5d^26s\ ^8I$	1.292	1.354	0.062
	25526		21.0	$4f^8(^7F)5d^26s\ ^8F$	10.4	$4f^8(^7F)5d^26s\ ^8G$	1.453		
25553.46	25560	−7	34.4	$4f^9(^6H)6s6p\ ^6H$	7.0	$4f^9(^6H)5d6p\ ^6H$	1.297	1.328	0.031
25717.68	25749	−31	17.2	$4f^8(^5L)5d6s^2\ ^6L$	15.4	$4f^9(^6F)6s6p\ ^8F$	1.239	1.300	0.061
	25833		33.9	$4f^8(^5L)5d6s^2\ ^6L$	6.2	$4f^9(^6F)6s6p\ ^8F$	1.084		
	26079		12.0	$4f^8(^7F)5d^26s\ ^8I$	10.3	$4f^9(^6F)6s6p\ ^8F$	1.316		
	26124		12.8	$4f^8(^7F)5d^26s\ ^8I$	8.9	$4f^8(^7F)5d^26s\ ^6G$	1.346		
	26300		16.2	$4f^8(^5L)5d6s^2\ ^6M$	12.3	$4f^8(^5G)5d6s^2\ ^6G$	1.133		
	26508		30.5	$4f^8(^7F)5d^3\ ^{10}H$	23.5	$4f^8(^7F)5d^3\ ^{10}G$	1.485		
26592.90	26606	−13	36.6	$4f^9(^6F)6s6p\ ^6G$	34.7	$4f^9(^6F)6s6p\ ^8G$	1.407		
	26745		34.8	$4f^8(^5L)5d6s^2\ ^6M$	11.4	$4f^8(^5L)5d6s^2\ ^6L$	0.901		
$J = 15/2$									
462.080	551	−89	85.9	$4f^8(^7F)5d6s^2\ ^8G$	4.2	$4f^8(^7F)5d6s^2\ ^8H$	1.457	1.456	−0.001
5425.060	5442	−17	64.9	$4f^8(^7F)5d6s^2\ ^8H$	20.3	$4f^8(^7F)5d6s^2\ ^6H$	1.375	1.370	−0.005
7767.015	7787	−20	67.2	$4f^8(^7F)5d6s^2\ ^6H$	21.7	$4f^8(^7F)5d6s^2\ ^8H$	1.343	1.342	−0.001
8190.465	8192	−2	62.2	$4f^8(^7F)5d^26s\ ^{10}G$	13.3	$4f^8(^7F)5d^26s\ ^{10}F$	1.532	1.540	0.008
11580.68	11579	1	42.7	$4f^8(^7F)5d^26s\ ^{10}F$	16.3	$4f^8(^7F)5d^26s\ ^{10}H$	1.519		
12628.67	12636	−7	27.7	$4f^8(^7F)5d^26s\ ^{10}H$	27.6	$4f^8(^7F)5d^26s\ ^{10}I$	1.455		
12932.66	12908	24	31.3	$4f^8(^7F)5d^26s\ ^8G$	18.2	$4f^8(^7F)5d^26s\ ^8G$	1.472		

Table 1. Continued.

$E_{\rm exp}$	$E_{\rm calc}$	ΔE	%	Main comp.	%	Sec. comp.	$g_{J\,\rm calc}$	$g_{J\,\rm exp}$	Δg_J
14569.67	14602	−32	41.8	$4f^8(^7F)5d^26s\ ^{10}I$	30.0	$4f^8(^7F)5d^26s\ ^{10}H$	1.398		
14888.11	14899	−11	44.1	$4f^9(^6H)6s6p\ ^8G$	17.5	$4f^9(^6H)6s6p\ ^8H$	1.400	1.391	−0.009
15387.79	15341	47	31.5	$4f^8(^7F)5d^26s\ ^8H$	15.2	$4f^8(^7F)5d^26s\ ^8I$	1.364	1.367	0.003
16343.30	16346	−2	32.2	$4f^9(^6H)6s6p\ ^4I$	19.5	$4f^9(^6H)6s6p\ ^6I$	1.274	1.397	0.123
16431.13	16474	−43	62.3	$4f^8(^7F)5d^26s\ ^{10}G$	12.0	$4f^8(^7F)5d^26s\ ^{10}G$	1.515	1.460	−0.055
	17169		21.9	$4f^8(^7F)5d^26s\ ^8H$	14.0	$4f^8(^7F)5d^26s\ ^6I$	1.338		
	17763		18.0	$4f^8(^7F)5d^26s\ ^6H$	17.8	$4f^9(^6H)6s6p\ ^6H$	1.324		
	18022		16.1	$4f^9(^6H)6s6p\ ^6H$	14.0	$4f^8(^7F)5d^26s\ ^6H$	1.324		
	18750		14.5	$4f^8(^7F)5d^26s\ ^8G$	14.1	$4f^8(^7F)5d^26s\ ^8G$	1.411		
	19177		21.6	$4f^9(^6H)6s6p\ ^8I$	20.5	$4f^9(^6H)6s6p\ ^8H$	1.325		
	19381		23.8	$4f^8(^7F)5d^26s\ ^8G$	22.4	$4f^8(^7F)5d^26s\ ^8G$	1.426		
	19724		15.7	$4f^8(^7F)5d^26s\ ^8H$	8.2	$4f^8(^7F)5d^26s\ ^8H$	1.432		
19920.41	19917	3	36.9	$4f^8(^7F)5d^3\ ^{10}F$	29.5	$4f^8(^7F)5d^3\ ^{10}F$	1.542		
	19949		16.2	$4f^8(^7F)5d^26s\ ^6I$	12.4	$4f^8(^7F)5d^26s\ ^{10}F$	1.352		
	20295		41.5	$4f^8(^7F)5d^26s\ ^{10}F$	9.5	$4f^8(^7F)5d^26s\ ^{10}F$	1.512		
	20406		26.2	$4f^8(^7F)5d^26s\ ^6H$	23.5	$4f^8(^7F)5d^26s\ ^4I$	1.306		
	21015		29.5	$4f^9(^6H)6s6p\ ^8H$	16.0	$4f^9(^6H)6s6p\ ^6I$	1.309		
	21113		17.3	$4f^8(^7F)5d^26s\ ^8I$	14.1	$4f^8(^7F)5d^26s\ ^8I$	1.356		
	21706		33.0	$4f^9(^6H)6s6p\ ^6H$	9.0	$4f^8(^7F)5d^26s\ ^8G$	1.348		
	21876		25.8	$4f^8(^7F)5d^26s\ ^8G$	16.6	$4f^9(^6H)6s6p\ ^6H$	1.402		
	22493		32.9	$4f^8(^7F)5d^3\ ^{10}H$	19.9	$4f^8(^7F)5d^3\ ^{10}I$	1.398		
	22535		27.1	$4f^8(^7F)5d^26s\ ^4I$	13.0	$4f^8(^7F)5d^3\ ^{10}H$	1.327		
	22767		24.2	$4f^8(^7F)5d^26s\ ^6H$	16.7	$4f^8(^7F)5d^26s\ ^6H$	1.316		
23031.84	23010	22	24.7	$4f^9(^6H)6s6p\ ^8I$	23.9	$4f^9(^6H)6s6p\ ^6I$	1.301	1.240	−0.061
23147.92	23220	−72	21.1	$4f^8(^7F)5d^26s\ ^8G$	18.1	$4f^8(^7F)5d^26s\ ^8H$	1.371	1.339	−0.032
	23259		19.3	$4f^8(^7F)5d^26s\ ^8H$	10.0	$4f^8(^7F)5d^26s\ ^8I$	1.327		
	23758		23.5	$4f^8(^5G)5d6s^2\ ^6H$	23.1	$4f^8(^5G)5d6s^2\ ^6H$	1.291		
	24309		20.3	$4f^8(^7F)5d^26s\ ^6I$	15.4	$4f^8(^7F)5d^26s\ ^6H$	1.309		
	24334		20.4	$4f^8(^7F)5d^26s\ ^8I$	12.6	$4f^8(^7F)5d^26s\ ^8H$	1.345		
	24384		51.3	$4f^8(^7F)5d^3\ ^{10}I$	24.2	$4f^8(^7F)5d^3\ ^{10}G$	1.433		
	25123		52.0	$4f^9(^6F)6s6p\ ^8G$	10.9	$4f^9(^6H)6s6p\ ^6I$	1.393		
	25156		23.4	$4f^8(^7F)5d^26s\ ^8I$	10.8	$4f^8(^7F)5d^26s\ ^8H$	1.342		
	25598		63.2	$4f^8(^5L)5d6s^2\ ^6L$	13.8	$4f^8(^5L)5d6s^2\ ^6M$	0.998		
25825.53	25803	23	15.2	$4f^9(^6H)6s6p\ ^6I$	9.9	$4f^9(^6F)6s6p\ ^8G$	1.324	1.246	−0.078
	25910		28.0	$4f^8(^7F)5d^3\ ^{10}H$	16.0	$4f^8(^7F)5d^3\ ^{10}G$	1.442		
	25971		17.1	$4f^8(^7F)5d^26s\ ^8G$	14.0	$4f^8(^7F)5d^26s\ ^6H$	1.434		
$J = 17/2$									
4646.830	4656	−9	90.1	$4f^8(^7F)5d6s^2\ ^8H$	2.5	$4f^8(^7F)5d^3\ ^8H$	1.407	1.406	−0.001
8506.710	8514	−8	72.9	$4f^8(^7F)5d^26s\ ^{10}G$	11.8	$4f^8(^7F)5d^26s\ ^{10}G$	1.517	1.530	0.013
11879.20	11882	−3	47.0	$4f^8(^7F)5d^26s\ ^{10}H$	31.4	$4f^8(^7F)5d^26s\ ^{10}I$	1.438	1.430	−0.008
14016.91	14031	−14	39.0	$4f^8(^7F)5d^26s\ ^{10}I$	30.2	$4f^8(^7F)5d^26s\ ^{10}H$	1.415		
14718.11	14739	−21	47.4	$4f^8(^7F)5d^26s\ ^8H$	14.7	$4f^8(^7F)5d^26s\ ^{10}I$	1.395	1.400	0.005
15189.26	15166	24	45.2	$4f^9(^6H)6s6p\ ^8H$	13.6	$4f^9(^6H)6s6p\ ^8I$	1.367	1.409	0.042
	15699		60.4	$4f^8(^7F)5d^26s\ ^{10}G$	15.8	$4f^8(^7F)5d^26s\ ^{10}G$	1.494		
	16766		31.8	$4f^8(^7F)5d^26s\ ^8I$	19.7	$4f^8(^7F)5d^26s\ ^8H$	1.361		

Table 1. Continued.

$E_{\rm exp}$	$E_{\rm calc}$	ΔE	%	Main comp.	%	Sec. comp.	$g_{J\,\rm calc}$	$g_{J\,\rm exp}$	Δg_J
17249.59	17260	−11	44.7	$4f^9(^6H)6s6p\ ^6I$	30.0	$4f^9(^6H)6s6p\ ^8H$	1.329		
	18798		27.9	$4f^8(^7F)5d^26s\ ^6I$	24.1	$4f^8(^7F)5d^26s\ ^8H$	1.355		
	19491		24.4	$4f^8(^7F)5d^26s\ ^8H$	21.9	$4f^8(^7F)5d^26s\ ^6I$	1.353		
	20287		18.3	$4f^8(^7F)5d^26s\ ^8I$	17.0	$4f^8(^7F)5d^26s\ ^8I$	1.356		
	20702		51.3	$4f^9(^6H)6s6p\ ^8I$	11.2	$4f^9(^6H)6s6p\ ^6I$	1.329		
	21413		35.5	$4f^9(^6H)6s6p\ ^6I$	12.6	$4f^8(^7F)5d^26s\ ^6I$	1.300		
	21854		45.9	$4f^8(^7F)5d^3\ ^{10}H$	26.2	$4f^8(^7F)5d^3\ ^{10}I$	1.447		
	22233		31.3	$4f^8(^7F)5d^26s\ ^8H$	10.0	$4f^8(^7F)5d^26s\ ^8I$	1.371		
	22875		36.7	$4f^8(^7F)5d^26s\ ^8H$	18.7	$4f^8(^7F)5d^26s\ ^8I$	1.373		
23107.25	23146	−39	34.0	$4f^8(^7F)5d^26s\ ^6I$	11.7	$4f^8(^7F)5d^26s\ ^8I$	1.307	1.289	−0.018
	23681		45.9	$4f^8(^7F)5d^3\ ^{10}I$	31.8	$4f^8(^7F)5d^3\ ^{10}G$	1.453		
	24512		33.6	$4f^8(^7F)5d^26s\ ^8I$	14.8	$4f^8(^7F)5d^26s\ ^8H$	1.347		
	24978		53.5	$4f^8(^5L)5d6s^2\ ^6L$	19.6	$4f^8(^5L)5d6s^2\ ^6K$	1.127		
$J = 19/2$									
11331.14	11313	18	65.8	$4f^8(^7F)5d^26s\ ^{10}H$	28.5	$4f^8(^7F)5d^26s\ ^{10}I$	1.451	1.460	0.009
13398.40	13395	3	56.7	$4f^8(^7F)5d^26s\ ^{10}I$	27.5	$4f^8(^7F)5d^26s\ ^{10}H$	1.422		
	15870		68.5	$4f^8(^7F)5d^26s\ ^8I$	11.8	$4f^8(^7F)5d^26s\ ^8I$	1.372		
	16792		86.6	$4f^9(^6H)6s6p\ ^8I$	7.1	$4f^9(^4I)6s6p\ ^6K$	1.358		
	20295		55.8	$4f^8(^7F)5d^26s\ ^8I$	29.6	$4f^8(^7F)5d^26s\ ^8I$	1.363		
	21715		48.5	$4f^8(^7F)5d^3\ ^{10}I$	44.5	$4f^8(^7F)5d^3\ ^{10}H$	1.436		
	22984		49.6	$4f^8(^7F)5d^26s\ ^8I$	20.9	$4f^8(^7F)5d^26s\ ^8I$	1.363		
$J = 21/2$									
12283.30	12248	36	95.2	$4f^8(^7F)5d^26s\ ^{10}I$	2.0	$4f^8(^5G)5d^26s\ ^8K$	1.425		
	21743		93.3	$4f^8(^7F)5d^3\ ^{10}I$	2.6	$4f^8(^5G)5d^3\ ^8K$	1.423		
	23610		69.4	$4f^8(^5L)5d6s^2\ ^6L$	13.0	$4f^8(^5L)5d6s^2\ ^6M$	1.215		
	24720		88.1	$4f^8(^7F)5d^26s\ ^8K$	4.2	$4f^8(^7F)5d^3\ ^8K$	1.330		
$J = 23/2$									
	24760		50.1	$4f^8(^5L)5d6s^2\ ^6M$	21.8	$4f^8(^5L)5d6s^2\ ^6N$	1.179		
$J = 25/2$									
	26160		88.0	$4f^8(^5L)5d6s^2\ ^6N$	4.1	$4f^8(^3M)5d6s^2\ ^4O$	1.194		
$J = 27/2$									
	33634		80.3	$4f^8(^5L)5d^26s\ ^8N$	11.8	$4f^8(^5L)5d^26s\ ^8O$	1.247		
$J = 29/2$									
	35024		92.4	$4f^8(^5L)5d^26s\ ^8O$	4.0	$4f^8(^3M)5d^26s\ ^6Q$	1.236		
$J = 31/2$									
	48950		50.9	$4f^8(^3O)5d^26s\ ^6T$	36.3	$4f^8(^3O)5d^26s\ ^6R$	1.125		

References

1. M. Elantkowska, J. Ruczkowski, J. Dembczyński, Eur. Phys. J. Plus **130**, 14 (2015).
2. M. Elantkowska, J. Ruczkowski, J. Dembczyński, Eur. Phys. J. Plus **130**, 15 (2015).
3. M. Elantkowska, J. Ruczkowski, J. Dembczyński, Eur. Phys. J. Plus **130**, 83 (2015).
4. M. Elantkowska, J. Ruczkowski, J. Dembczyński, Eur. Phys. J. Plus **130**, 170 (2015).
5. M. Elantkowska, J. Ruczkowski, J. Dembczyński, Eur. Phys. J. Plus **131**, 47 (2016).
6. M. Elantkowska, J. Ruczkowski, J. Dembczyński, Eur. Phys. J. Plus **131**, 429 (2016).
7. J. Dembczyński, M. Elantkowska, K. Bekk, H. Rebel, M. Wilson, Z. Phys. D **13**, 181 (1989).
8. M. Elantkowska, A. Bernard, J. Dembczyński, J. Ruczkowski, Z. Phys. D **27**, 103 (1993).
9. E. Stachowska, M. Elantkowska, J. Ruczkowski, J. Dembczyński, Phys. Scr. **65**, 237 (2002).
10. J. Ruczkowski, E. Stachowska, M. Elantkowska, G.H. Guthöhrlein, J. Dembczyński, Phys. Scr. **68**, 133 (2003).
11. B. Furmann, D. Stefanska, A. Krzykowski, Spectrochim. Acta Part B **111**, 38 (2015).
12. B. Furmann, D. Stefanska, A. Krzykowski, J. Phys. B **49**, 025001 (2016).
13. D. Stefanska, M. Elantkowska, J. Ruczkowski, B. Furmann, J. Quantum Spectrosc. Radiat. Transf. **189**, 441 (2017).
14. Z.G. Zhang, S. Svanberg, P. Palmeri, P. Quinet, E. Biemont, Mon. Not. R. Astron. Soc. **334**, 1 (2002).
15. R.D. Cowan, *The Theory of Atomic Structure and Spectra* (Berkeley University of California Press, Berkeley, 1981).
16. R.D. Cowan, *Robert D. Cowan's Atomic Structure Code*, available on-line at the following link: `https://www.tcd.ie/Physics/people/Cormac.McGuinness/Cowan/`.
17. P. Quinet, E. Biémont, Mon. Not. R. Astron. Soc. **340**, 463 (2003).
18. J.-F. Wyart, W.-Ü.L. Tchang-Brillet, S.S. Churilov, A.N. Ryabtsev, Astron. Astrophys. **483**, 339 (2008).
19. M. Macy *et al.*, available on-line: `https://docs.microsoft.com/pl-pl/azure/batch/batch-mpi`.
20. A. Kramida, Yu. Ralchenko, J. Reader, NIST ASD Team, *NIST Atomic Spectra Database* (ver. 5.3), available on-line: `http://physics.nist.gov/asd` (National Institute of Standards and Technology, Gaithersburg, MD, 2016).
21. W.C. Martin, R. Zalubas, L. Hagan, *Atomic energy levels – The rare-earth elements*, in Nat. Stand. Ref. Data Ser., NSRDS-NBS 60, Nat. Bur. Stand., U.S. (1978).